

Positron-annihilation study of equilibrium defects in Al-Cu-Fe face-centered-icosahedral quasicrystals

D. W. Lawther* and R. A. Dunlap

Department of Physics, Dalhousie University, Halifax, Nova Scotia, Canada B3H 3J5

(Received 23 April 1993; revised manuscript received 27 September 1993)

In situ Doppler-broadening temperature scans and room temperature positron-lifetime measurements are reported for $\text{Al}_{63}\text{Cu}_{25}\text{Fe}_{12}$, $\text{Al}_{62.5}\text{Cu}_{25}\text{Fe}_{12.5}$, $\text{Al}_{62}\text{Cu}_{25.5}\text{Fe}_{12.5}$, and $\text{Al}_{62}\text{Cu}_{22.8}\text{Fe}_{15.2}$ face-centered-icosahedral (FCI) quasicrystalline samples. Quenched-in disorder has been observed and found to anneal out of the samples above 200 °C. A quasicrystal-to-microcrystal phase transition has been observed in two of the samples ($\text{Al}_{63}\text{Cu}_{25}\text{Fe}_{12}$ and $\text{Al}_{62}\text{Cu}_{22.8}\text{Fe}_{15.2}$), indicating an instability of the FCI phase at low temperatures. No such transition is observed in the other two samples ($\text{Al}_{62.5}\text{Cu}_{25}\text{Fe}_{12.5}$ and $\text{Al}_{62}\text{Cu}_{25.5}\text{Fe}_{12.5}$). It is shown that intrinsic structural vacancies, possessing only Al-atom nearest neighbors, exist in both the microcrystal and FCI phases and act as saturation traps for the positrons. At ~ 200 °C, thermal activation of dynamic Al-atom phasons in the FCI phase results in distortions of the intrinsic structural vacancies as the nearest neighbor Al atoms begin to hop within double-well potentials. At higher temperatures (525–750 °C depending upon the sample stoichiometry) dynamic Cu-atom phasons are activated and observed to coincide with the onset of plasticity in the FCI phase.

I. INTRODUCTION

The stable face-centered icosahedral (FCI) phase in Al-Cu-Fe was the first quasicrystal to be discovered with little or no phason disorder.^{1,2} It is therefore not surprising that it is also the most extensively studied. Experimental results from investigations of the structural (e.g., Refs. 3–8), thermal (e.g., Refs. 9–15), electrical (e.g., Refs. 16–23), dynamic,^{24–28} and mechanical^{29–31} properties have all been reported.

The physical properties have been shown to be highly sensitive to sample composition^{32,33} and thermal history.³⁴ For example, the FCI phase extends only over a few atomic percent in composition at elevated temperatures.¹² As the temperature is reduced, this region contracts toward a higher Fe content but remains finite. At room temperature, it is centered on the composition $\text{Al}_{62.3}\text{Cu}_{24.9}\text{Fe}_{12.8}$. For a given stoichiometry, the FCI phase generally transforms upon cooling into a complex mixture of microcrystalline structures characterized by fine diffraction effects (peak broadening, line shapes, etc.). Thus the resulting phase(s), and in particular, the defect structures, are expected to depend quite sensitively upon the details of the sample preparation.

Positron-annihilation investigations of the defect structures in Al-Mn-Si (Refs. 35–40) and Al-Li-Cu (Refs. 40–43) simple icosahedral (SI) as well as Al-Cu-Fe FCI (Refs. 44–50) quasicrystals have appeared in the literature.

In the case of the SI quasicrystals, their close association with crystalline approximants [i.e., α -Al-Mn-Si (Ref. 51) and R -Al-Li-Cu (Ref. 52)] has been exploited to show that the positrons experience saturation trapping within intrinsic structural vacancies. These approximant structures are known to consist of a bcc packing of atomic clusters with icosahedral symmetry: a 54-atom

Mackay icosahedron (MI) in the case of α -Al-Mn-Si and a 44-atom rhombic triacontahedron in the case of R -Al-Li-Cu. The central site of these two clusters is vacant and thus offers an ideal positron trap. Presumably, the corresponding SI structures possess an alternative packing of these same clusters (allowing for possible distortion).

The reported positron-lifetime spectra for the Al-Cu-Fe FCI phase^{45–47,49,50} reveal the existence of two components: (1) a principal lifetime, $\tau_1 \sim 150$ –200 psec, generally ascribed to positrons annihilating from the bulk (i.e., not localized within a defect), and (2) $\tau_2 \sim 240$ –400 psec, corresponding to positrons annihilating from within vacancies or voids. The persistence of this second component, even after heat treatment up to 400 °C, has led Chidambaram *et al.*^{45,50} to suggest that the Al-Cu-Fe FCI structure is best described as a form of icosahedral glass.⁵³ However, this is contrary to the overwhelming quasicrystallographic data (e.g., Refs. 3–7) which indicate near perfect quasiperiodic ordering. Unfortunately, in this latter case, specific information regarding site vacancies is not readily obtainable.

To date, no justification has been given for either the observation of the nonlocalized component or its corresponding lifetime value in the Al-Cu-Fe FCI phase. Although no analogous approximant structure for the Al-Cu-Fe FCI phase has yet been determined, a 1/1 cubic approximant, isostructural with α -Al-Mn-Si, has been reported for the Al-Cu-Ru FCI quasicrystal.⁵⁴ Furthermore, DiVincenzo *et al.*⁸ have proposed a cluster model based upon interpenetrating MI for the Al-Cu-Fe FCI structure. Three different interpenetration schemes are identified, resulting in perhaps only partial occupation of the cluster centers with a Cu atom from an adjacent cluster.

In this paper, results from Doppler-broadening (DB) and positron-lifetime measurements on a number of Al-

Cu-Fe samples as a function of temperature and sample thermal treatment are presented. The chosen stoichiometries and methods of sample preparation reflect those which have been previously reported in the literature. The aim of this work is to (a) clarify the effect of various thermal treatments on the formation of quenched-in defects, (b) determine the occurrence and identity of equilibrium defect formation (including the possible occurrence of an intrinsic structural vacancy), and (c) correlate the defect formation to behavior observed from other studies (i.e., scattering, electron transport, compression testing, etc.) which have appeared in the literature for the Al-Cu-Fe FCI quasicrystals.

II. EXPERIMENTAL DETAILS

Polycrystalline samples of nominal stoichiometry $\text{Al}_{63}\text{Cu}_{25}\text{Fe}_{12}$ (sample A), $\text{Al}_{62.5}\text{Cu}_{25}\text{Fe}_{12.5}$ (sample B), and $\text{Al}_{62}\text{Cu}_{25.5}\text{Fe}_{12.5}$ (sample C) were prepared by melting high purity elemental components in an argon arc furnace. The ingots were crushed, sieved through a 120 μm mesh, sealed under argon in quartz tubes, and annealed for 24 h at 800 °C. A temperature of 800 °C is required to ensure the annealing out of quenched-in impurity phases and nonequilibrium residual disorder.³⁴ The subsequent cooling procedure is discussed below.

Single crystals of $\text{Al}_{62}\text{Cu}_{22.8}\text{Fe}_{15.2}$ (sample D) were prepared by the method described by Ishimasa and Mori.⁵⁵ In this case, the above procedure was repeated except that the powdered sample was annealed 12 h at 870 °C followed by slow cooling (<2 °C/h) to 820 °C at which the sample was further annealed for 24 h. The initial anneal stage results in sintering of the powder, whereas compositional inhomogeneities develop in association with the growth of large grains of the FCI phase during the slow cooling. The final anneal stage allows for the removal of quenched-in disorder in the grains. Single crystals (with dimensions of a few mm and masses ranging from 10 to 20 mg) of the FCI phase were then cut from the ingot.

The stoichiometries of samples A and D are both known to yield stable quasicrystals only at elevated temperatures.^{9,55} Slow cooling from such temperatures leads to the production of phason disorder which tends to modulate the structure into complex arrays of microcrystalline particles.¹² For this reason, samples A and D were ice-water quenched from their final anneal temperature. The stoichiometries of samples B and C correspond closely to that for which the quasicrystalline phase is known to be stable over the entire temperature range up to the solidus.⁹ These samples were therefore slow cooled (<100 °C/h) from their final anneal temperature.

Room-temperature x-ray powder diffraction analysis was performed using Cu $K\alpha$ radiation on a Siemens D-500 scanning diffractometer. A typical diffraction pattern for the as-prepared samples is shown in Fig. 1. For sample D, a single grain cut from the ingot was crushed and the x-ray analysis was performed on the resulting powder. All four samples showed the existence of a pure FCI phase although peak broadening was observed for samples A and D.

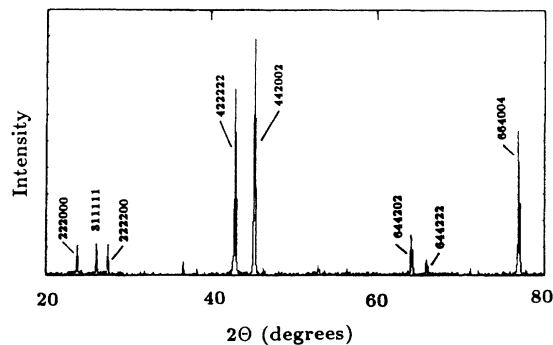


FIG. 1. Room-temperature x-ray powder diffraction spectrum for as-prepared $\text{Al}_{62}\text{Cu}_{25.5}\text{Fe}_{12.5}$ (sample C). All the peaks are indexed to the FCI phase; however, only the principal peaks have been labeled in the figure.

DB measurements were performed using an EG&G ORTEC GEM-20190 HPGe detector (22% efficiency at 1.33 MeV) with an energy resolution of (1.25 ± 0.02) keV full width at half maximum (FWHM) at 497 keV. The positron source for the *in situ* temperature scans was produced by vacuum sealing approximately 100 mg of the as-prepared samples in quartz followed by thermal neutron irradiation [$^{63}\text{Cu}(n, \gamma)^{64}\text{Cu}$]. Typical irradiation times of 10 min with a flux of 5.4×10^{-13} neutrons/barn sec were employed. After a subsequent delay of several hours (to allow for the decay of short-lived activity from ^{28}Al and ^{66}Cu) the sealed samples were inserted into a furnace mounted above the detector on a translational (vertical) stage. Each measurement required 10 min, during which, the temperature was controlled to within ± 1 °C. To compensate for the drop in the ^{64}Cu activity (a typical temperature scan required approximately one full half-life of ^{64}Cu to complete), the sample-detector distance was periodically adjusted.

The DB spectra were stripped of their background and characterized by the line-shape parameter

$$L = \sum_{i=-n}^n K_i / \left(\sum_{i=-n}^{-m} K_i + \sum_{i=n}^m K_i \right), \quad m > n, \quad (1)$$

where K_i is the number of counts corresponding to channel (energy) i , $i=0$ corresponds to the peak centroid, and n and m are chosen to encompass the immediate region around the centroid and the wing areas, respectively.

The positron-lifetime apparatus consisted of a fast-timing coincidence system using CsF crystals mounted on Hamamatsu H2431 PMT assemblies. A time resolution of 350 psec was measured using the prompt peak of ^{60}Co . A conventional sample/source/sample sandwich geometry was used⁴⁸ with the source inserted into a plastic holder with 1 cm \times 1 cm \times 2.5 mm thick sample compartments. The source was prepared by evaporating ^{22}Na (\sim few μCi) onto a 0.011 mm thick sheet of kapton and covering with a second sheet of the same.

Room-temperature positron-lifetime measurements were performed on samples A, B, and C after various isochronal anneal treatments. The mass of the single crystal (sample D) was not sufficient to perform the

positron-lifetime measurements. Each isochronal anneal was for 12 h at the temperature, T_a , followed by either slow cooling ($<100^\circ\text{C/h}$) or ice-water quenching. The set of anneals on a given sample was done on the entire batch and the subsequent measurements performed on a random portion of it. Before each anneal, the sample was sealed in a quartz tube under 0.5 atm of argon. Before each measurement, the samples were sieved to $<120\ \mu\text{m}$ to ensure constancy of the filling fraction in the sample holder. In all cases, the total mass of sample used was $\sim 750\ \text{mg}$.

The lifetime spectra were fitted to one and two components after extraction of the background and source component using an algorithm based on that described by Kirkegaard and Eldrup.⁵⁶

All the measurement results reported in the next section were confirmed by repeating the experiments on a second batch of samples prepared by the identical procedures.

III. RESULTS

Figures 2 and 3 show L as a function of temperature for the *in situ* DB measurements on the four samples. Table I summarizes the results from the room-temperature positron-lifetime measurements. The following general features are observed.

(1) The positron-lifetime spectra are generally comprised of two components: (1) a principal component with lifetime, $\tau_1 \sim 195\ \text{psec}$, and (2) a lower intensity

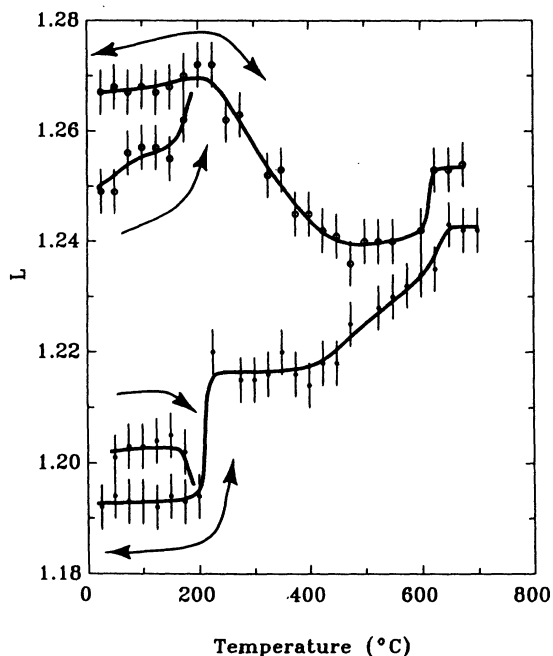


FIG. 2. L parameter values from *in situ* Doppler-broadening measurements on polycrystalline (○) $\text{Al}_{63}\text{Cu}_{25}\text{Fe}_{12}$ (sample A) and (●) $\text{Al}_{62}\text{Cu}_{25.5}\text{Fe}_{12.5}$ (sample C). The lines drawn through the points are only guides and do not represent fits to a model. The single headed arrows correspond to the initial heating whereas the double headed arrows correspond to subsequent thermal cycling.

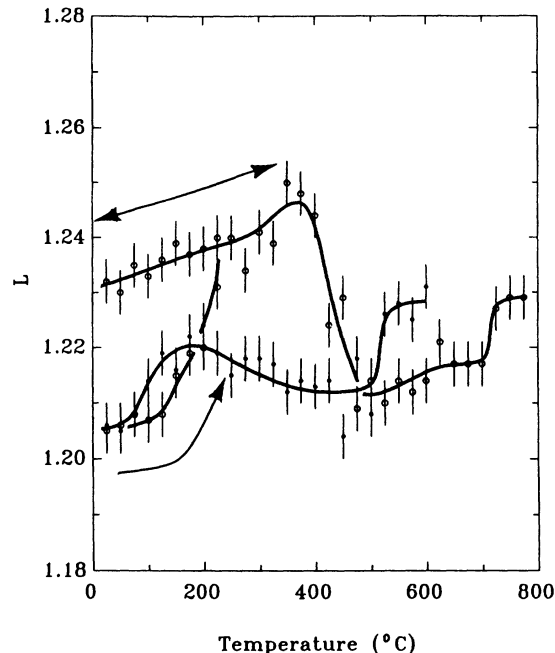


FIG. 3. L parameter values from *in situ* Doppler-broadening measurements on single crystal (○) $\text{Al}_{62}\text{Cu}_{22.8}\text{Fe}_{15.2}$ (sample D) and polycrystalline (●) $\text{Al}_{62.5}\text{Cu}_{25}\text{Fe}_{12.5}$ (sample B). The lines drawn through the points are only guides and do not represent fits to a model. The single headed arrow corresponds to the initial heating whereas the double headed arrow corresponds to subsequent thermal cycling.

TABLE I. Results from one- and two-component fits to Al-Cu-Fe positron-lifetime spectra corrected for source contributions. All thermal treatments involved annealing at the specified temperatures for 12 h followed by either slow cooling (SC) or ice-water quenching (IWQ). $\bar{\tau}$ is the mean lifetime and I_2 is the relative intensity of the second lifetime component, τ_2 , in the two-component fit. VOF is the variance-of-fit value.

Thermal treatment	$\bar{\tau}$ [ps]	τ_1 [ps]	τ_2 [ps]	I_2 [%]	VOF
$\text{Al}_{63}\text{Cu}_{25}\text{Fe}_{12}$ (sample A)					
SC 200 °C	214(2)	196(2)	403(10)	21(5)	1.1
SC 530 °C	214	195	393	21	1.2
IWQ 530 °C	206	193	300	10	1.2
$\text{Al}_{62.5}\text{Cu}_{25}\text{Fe}_{12.5}$ (sample B)					
SC 200 °C	195	190	227	15	1.3
SC 530 °C	190	181	242	19	1.2
IWQ 530 °C	198	192	235	15	1.2
$\text{Al}_{62}\text{Cu}_{25.5}\text{Fe}_{12.5}$ (sample C)					
SC 200 °C	194	-	-	-	1.0
SC 530 °C	190	180	270	18	1.2
IWQ 530 °C	196	193	237	8	1.0

second component with lifetime, τ_2 , in the range 230 – 270 psec or 300–400 psec. For sample C annealed at 200 °C, only the principal component is observed.

(2) A broad peak in the temperature dependence of L is observed for samples A and D extending from room temperature to about 450 °C. The positron-lifetime measurements (Table I) on sample A show that this elevation in L corresponds to an increase in both τ_2 and I_2 .

(3) A broad peak in the temperature dependence of L is also observed for sample B (Fig. 3), although the elevation in L is not as great as for samples A and D. No significant change in either τ_2 or I_2 (Table I) is observed to correspond to this elevation in L .

(4) For sample C no such peak is observed. Instead, a step occurs at about 225 °C (Fig. 2). Lifetime measurements on the sample after annealing and quenching from above and below this step show that the elevation in L corresponds to the generation of a second component with a lifetime (τ_2) of ~ 250 psec (Table I).

(5) Nonequilibrium behavior is observed in the as-prepared states of samples A, C, and D (Figs. 2 and 3). Reversion to equilibrium (i.e., reversible) behavior is observed after heating the samples above ~ 200 °C.

(6) In all four samples, a high temperature step is observed for L between about 525 and 750 °C depending upon the stoichiometry (Figs. 2 and 3). For sample C, this step is preceded by a general increase in L as the temperature increases from 400 to 625 °C.

IV. DISCUSSION

The existence of two components in the positron-lifetime spectra has been interpreted in previous studies^{45,50} in terms of a simple two-state trapping model. The positrons are assumed to annihilate from either the bulk state (τ_1) or a localized state from within a vacancy (τ_2). However, the principal lifetime, $\tau_1 \sim 195$ psec, observed here cannot be derived from positrons annihilating from the bulk state. Approximating the expected bulk positron lifetime in the Al-Cu-Fe FCI quasicrystal to be the compositionally weighted average of the constituent element values [$\tau_{\text{Al}} = 163$ psec, $\tau_{\text{Cu}} = 110$ psec, and $\tau_{\text{Fe}} = 106$ psec (Ref. 57)], the determined value of ~ 140 psec is significantly shorter than the observed τ_1 value.

On the other hand, there is now considerable evidence (e.g., Ref. 16) to support the suggestion that the stable FCI quasicrystals are electron compounds (i.e., Hume-Rothery compounds). Interaction of the Fermi surface with a pseudozone formed by a set of Bragg planes (corresponding to the most intense x-ray Bragg peaks: 422222 and 442002 in Fig. 1), implies

$$2|\mathbf{k}|_F \sim |\mathbf{G}|, \quad (2)$$

where $|\mathbf{k}|_F$ and $|\mathbf{G}|$ are the magnitudes of the Fermi wave vector and reciprocal lattice vector, respectively. Assuming a spherical Fermi surface,

$$|\mathbf{k}|_F = (3\pi^2 n_e)^{1/3}, \quad (3)$$

where $n_e = (e/a)n_a$ is the free-electron density and n_a

is the atomic density. Since the mass density of the Al-Cu-Fe quasicrystals has been determined to be ~ 4.5 g/cm³ (Ref. 58) and $|\mathbf{G}| = 3.094 \text{ \AA}^{-1}$ (Ref. 59) for Al₆₂Cu_{25.5}Fe_{12.5} (sample C), $n_e = 1.25 \times 10^{23} \text{ cm}^{-3}$, and $e/a = 1.84$ electrons/atom. Note that this e/a value is close to 1.78 electrons/atom which is calculated on the basis of a valence of +3, +1, and -2.66 (Pauling charge transfer⁶⁰) for Al, Cu, and Fe, respectively.

In electrically conductive materials, an upper limit of $\tau_\infty \sim 500$ psec ($=1/\lambda_\infty$) (irrespective of whether the positrons annihilate from within a vacancy or not) results from a weighted average of the annihilation rates of para- and ortho-positronium. This implies that⁶¹ the bulk lifetime

$$\tau_b = [\lambda_\infty(1 + \lambda_b)]^{-1}. \quad (4)$$

A recent consideration of the systematic variation of τ_b in alkali metals and polyvalent metals without d electrons has resulted in the empirical relation,⁵⁷

$$\lambda_b = (22.6n_e V_B)^{0.78}, \quad (5)$$

where $V_B = 4\pi a_B^3/3$ and a_B is the Bohr's radius ($=5.292 \times 10^{-11}$ m). The bulk annihilation rates are plotted with respect to $n_e V_B$ in Fig. 4.

For sample C, Eq. (5) gives $\tau_b = 196$ psec which is in good agreement with the experimentally determined τ_1 value (Fig. 4). In general, transition metals tend to fall above this line while semimetals and semiconductors tend to fall below this line. This indicates that τ_1 from the positron-lifetime fits corresponds to positron annihilation with the conduction electrons (i.e., not the d electrons).

This result is incompatible with the previous assumption that the positrons are primarily in an extended bulk state at the time of annihilation. If this were the case, the significant d -orbital character of the Al-Cu-Fe FCI quasicrystals would influence the annihilation parameters.

The explanation is that the positrons are highly localized in Al-rich regions of the atomic structure. This

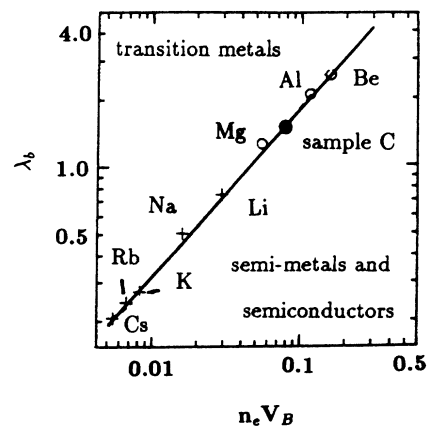


FIG. 4. Bulk annihilation rates, λ_b , for the alkali metals (+) and the polyvalent metals without d electrons (\circ) vs $n_e V_B$ (adapted from Ref. 57). The solid line corresponds to Eq. (5) in the text. Also included in the figure is the result for Al₆₂Cu_{25.5}Fe_{12.5} (sample C) (\bullet).

would exclude overlap of the positron wave function with those of the Cu and Fe *d* electrons. The most likely candidate for such sites are vacant cluster centers surrounded by an icosahedral coordination of Al atoms. The stability of the τ_1 value over varying stoichiometry and thermal treatment (see Table I) lends further support for the suggestion that the sites are intrinsic structural vacancies.

The observation of a single lifetime component in sample C indicates that saturation trapping of the positrons occurs within these intrinsic structural vacancies. The simple two-state trapping model is therefore not applicable.

Figures 2 and 3 and Table I clearly illustrate the need for care when reporting the thermal history of the sample under investigation (e.g., compare the results from the initial heating of the as-prepared samples to that from subsequent thermal cycling). In particular, slow cooling ($<100^\circ\text{C}/\text{h}$) sample C still resulted in quenched-in vacancy disorder (as evidenced by elevated L , I_2 , and τ_2 values). In each case, the nonequilibrium behavior is removed after annealing the sample at $\sim 200^\circ\text{C}$.

The positron-annihilation measurements show that equilibrium vacancies are present in the Al-Cu-Fe samples over the entire temperature range investigated. In fact, only below about 200°C for sample C was there a failure to observe a second lifetime component.

There is no doubt that the longer-lived τ_2 is associated with the formation of an open volume defect. The significant variance in both I_2 and τ_2 indicates that this second component does not correspond to a stable intrinsic structural vacancy. It is possible that τ_2 can be ascribed to a distortion of a fraction of the intrinsic vacancies or to the formation of a distinct form of defect. The correct interpretation is likely to be sample specific.

The *in situ* DB measurements show an elevation of the line-shape parameter for samples A and D as the temperature is lowered (Figs. 2 and 3). This can be associated with a low temperature instability of the FCI quasicrystalline phase in both of these samples. Positron-lifetime measurements on sample A (Table I) show that this corresponds to an increase in I_2 and τ_2 to about 20% and

400 psec, respectively. The *in situ* DB temperature scans indicate a crystallization temperature of $425\text{--}450^\circ\text{C}$ (Table II) in the two samples.

Ice-water quenching from above the crystallization temperature, T_{cryst} , appears to be only partially successful in preventing the transformation process. Evidence for this comes from the relatively high value for L at room temperature for the as-prepared sample A compared to that above T_{cryst} (Fig. 2).

It has been shown that the microcrystalline morphology of the transformed phase consists of oriented grains^{62,63} with dimensions of less than a few hundred angstroms.¹¹ Such a transformation results in the appearance of diffuse scattering and low intensity shoulder peaks about the principal powder diffraction peaks of the FCI phase (see, e.g., Ref. 11). These same features have been observed in the case of sample A (Ref. 48) and D. It is therefore concluded that the positrons are becoming trapped at the microcrystallite boundaries.

The precise nature of these boundary-trap sites is not known. High resolution electron microscopy (HREM) studies^{11,62} have indicated that the interfacial regions are coherent. On the other hand, the pronounced temperature dependence of L for the microcrystalline phase (samples A and D in Figs. 2 and 3, respectively) suggests that the traps are extended in one or more dimensions.⁶⁴

The stoichiometries of samples B and C have been shown to produce a stable FCI quasicrystal over the entire temperature range up to the solidus.⁹ X-ray powder diffraction analysis of these two samples failed to show the formation of the peak structure observed for samples A and D. The absence of a pronounced elevation in L and τ_2 for low temperature anneals (Figs. 2, 3, and Table I) confirms this result.

The second component lifetime, $\tau_2 \sim 240$ psec, found for both samples B and C is significantly lower than that observed in samples A and D. Furthermore, it appears for sample C only after annealing above $\sim 200^\circ\text{C}$ and does not induce a noticeable change in the x-ray powder diffraction spectra. This implies the existence of a positron-trap site other than the extended intergrain site found for the microcrystalline phase.

It is not likely that a vacancy cluster, large enough to produce a $\tau \sim 240$ psec (the intrinsic structural vacancy, with $\tau \sim 195$ psec, is expected to be approximately a monovacancy in size), would be thermally generated at 200°C . A least-squares fit of the low temperature L values for sample C to a two-state trap model yields an enthalpy of vacancy formation in the range $0.6\text{--}0.8$ eV.

Time-of-flight quasielastic neutron scattering experiments have recently been performed as a function of temperature on an $\text{Al}_{62}\text{Cu}_{25.5}\text{Fe}_{12.5}$ sample.^{24,25,28} Broadening of the quasielastic component occurs above 650°C . This effect has been ascribed to cooperative phason hopping of Al and Cu atoms. The participating Cu atoms are presumed to occupy a fraction of the atomic cluster centers from which a phason hop to an unoccupied site beyond the inner icosahedral shell of Al atoms occurs. This process is assisted by a cooperative phason hop of an Al atom from the icosahedral shell to its alternate site within a double-well potential.²⁴ The Al phason

TABLE II. Temperature regimes for crystalline phase formation ($< T_{\text{cryst}}$) and plasticity ($> T_{\text{plastic}}$) as observed by the *in situ* Doppler-broadening measurements.

Sample	T_{cryst} [$^\circ\text{C}$]	T_{plastic} [$^\circ\text{C}$]
$\text{Al}_{63}\text{Cu}_{25}\text{Fe}_{12}$ (sample A)	425–450	600–630
$\text{Al}_{62.5}\text{Cu}_{25}\text{Fe}_{12.5}$ (sample B)	–	525–550
$\text{Al}_{62}\text{Cu}_{25.5}\text{Fe}_{12.5}$ (sample C)	–	625–640
$\text{Al}_{62}\text{Cu}_{22.8}\text{Fe}_{15.2}$ (sample D)	425–450	725–750

thus acts as a depinning mechanism for the Cu phason with a measured depinning energy of 0.75 eV.

It is therefore likely that the observed step in the L value for sample C at ~ 200 °C corresponds to the activation of dynamic Al phasons. Displacement of an Al atom would open up the close-packed icosahedral shell, distorting the intrinsic structural vacancy. This would further localized the positron wave function within a deeper potential well, decreasing the integrated positron-electron wave-function overlap and thus increasing the positron lifetime. It should be noted that the increase in the positron lifetime (~ 45 psec) is close to that observed for a divacancy compared to a monovacancy in Al.⁶⁵

The general increase in L for sample C above 400 °C is not readily interpreted. It is perhaps significant to note, however, that a plateau in the L behavior is reached at ~ 640 °C. This is typically the result of saturation of the positron within one of two (or more) competing states. As the temperature is increased, one of the states (usually corresponding to a positron-localizing defect) begins to dominate (e.g., thermal generation of a higher concentration of a specific type of defect) until a temperature is reached above which annihilations occur exclusively from that state. It is therefore likely that the elevation in L for sample C above ~ 400 °C corresponds to the introduction of an increasing concentration of a second positron trap state. The neutron scattering results (discussed above) suggest that the most likely candidate for this trap is associated with the generation of dynamic Cu-atom phasons. The discrepancy in the onset temperature (~ 400 °C from the positron results and ~ 650 °C from the neutron scattering results, respectively) reflects the greater sensitivity of the positron-annihilation technique to the detection of low defect concentrations.

Evidently the failure to observe a low temperature step for L in sample B implies that static phason disorder is locked into this sample at room temperature.

The observation of a high temperature step in L for samples A, B, and D (525 °C $< T < 750$ °C) may indicate that a similar dynamic Cu-atom phason occurs in each. The failure to observe a gradual increase in L (as is the case for sample C) may be associated with the presence of static phason disorder not present in sample C. This could also explain the observed dependence of the step temperature on sample stoichiometry.

A further comparison can be made to the results from recent compression tests³¹ on Al-Cu-Fe FCI quasicrystals which show a brittle-to-plastic transformation. In the case of sample A, the step temperature occurs between 600 and 630 °C which corresponds well to the reported temperature of 604 °C for the onset of plasticity, T_{plastic} (Ref. 31) (for a sample with the same stoichiometry). Any change in the structure responsible for the plasticity is expected to correspond to a significant change in the defect structure. This should be observed in the positron measurements. Since no other anomaly is observed in the temperature dependence of L (in the temperature region of interest), this step must correspond to T_{plastic} . The temperature regimes, derived from Figs. 2 and 3, corresponding to the activation of phase plasticity, $> T_{\text{plastic}}$, are summarized in Table II.

V. CONCLUSIONS

Equilibrium vacancy formation and behavior in Al-Cu-Fe FCI quasicrystals have been identified and categorized according to observed features from electron microscopy, x-ray diffraction, neutron scattering, and compression testing studies. Annealing of quenched-in disorder as well as the presence of a quasicrystal-to-microcrystal phase transition has been observed. Both the FCI phase and the microcrystalline phase have been found to possess an intrinsic structural vacancy characterized by Al-atom nearest neighbors. This site forms a saturation trap for the positrons. Thermal activation of Al and Cu dynamic phasons has been observed to distort the intrinsic structural vacancy in the FCI phase. The onset of plasticity in the FCI phase is found to coincide with the generation of the dynamic Cu-atom phasons.

ACKNOWLEDGMENTS

This work was supported by a grant from the Natural Sciences and Engineering Research Council of Canada. One of the authors (D.W.L.) is grateful for financial support from the I. W. Killam foundation. We also wish to thank Dr. I. K. MacKenzie for the use of his equipment and Dr. Z. J. Yang and S. P. Ritcey for useful suggestions during the preparation of the manuscript.

*Present address: Department of Physics, University of Western Ontario, London, Ontario, Canada N6A 3K7.

¹A.P. Tsai, A. Inoue, and T. Masumoto, *J. Mater. Sci. Lett.* **6**, 1403 (1987).

²A.P. Tsai, A. Inoue, Y. Yokoyama, and T. Masumoto, *Philos. Mag. Lett.* **61**, 9 (1990).

³Y. Calvayrac, A. Quivy, M. Bessière, S. Lefebvre, M. Cornier-Quiquandon, and D. Gratias, *J. Phys. (Paris)* **51**, 417 (1990).

⁴A. Katz and D. Gratias, *Phys. Rev. B* **44**, 2071 (1991).

⁵R. Bellissent, B. Mozer, Y. Calvayrac, D. Gratias, and J.W.

Cahn, *J. Non-Cryst. Solids* **153-154**, 1 (1993).

⁶M. Cornier-Quiquandon, R. Bellissent, Y. Calvayrac, J.W. Cahn, D. Gratias, and B. Mozer, *J. Non-Cryst. Solids* **153-154**, 10 (1993).

⁷X.B. Kan, J.L. Robertson, S.C. Moss, J. Kulik, T. Ishimasa, M. Mori, A. Quivy, D. Gratias, V. Elser, and P. Zschack, *J. Non-Cryst. Solids* **153-154**, 33 (1993).

⁸D.P. DiVincenzo, W. Krakow, P.A. Bancel, E. Cockayne, and V. Elser, *J. Non-Cryst. Solids* **153-154**, 145 (1993).

⁹M. Bessière, A. Quivy, S. Lefebvre, J. Devaud-Rzepski, and Y. Calvayrac, *J. Phys. France I* **1**, 1823 (1991).

- ¹⁰C. Janot, M. Audier, M. de Boissieu, and J.M. Dubois, *Europhys. Lett.* **14**, 355 (1991).
- ¹¹M. Audier, Y. Brechet, M. de Boissieu, P. Guyot, C. Janot, and J.M. Dubois, *Philos. Mag. B* **63**, 1375 (1991).
- ¹²A. Quivy and P.A. Bancel, *J. Non-Cryst. Solids* **153-154**, 482 (1993).
- ¹³M. Audier, P. Guyot, M. de Boissieu, and N. Menguy, *J. Non-Cryst. Solids* **153-154**, 591 (1993).
- ¹⁴F. Dénoyer, P. Launois, T. Motsch, and M. Lambert, *J. Non-Cryst. Solids* **153-154**, 595 (1993).
- ¹⁵A. Waseda, K. Araki, K. Kimura, and H. Ino, *J. Non-Cryst. Solids* **153-154**, 635 (1993).
- ¹⁶S.J. Poon, *Adv. Phys.* **41**, 303 (1992).
- ¹⁷E. Belin and Z. Danhkázi, *J. Non-Cryst. Solids* **153-154**, 298 (1993).
- ¹⁸R. Haberkern, P. Lindqvist, and G. Fritsch, *J. Non-Cryst. Solids* **153-154**, 303 (1993).
- ¹⁹T. Klein, C. Berger, G. Fourcaudot, J.C. Grieco, and J.C. Lasjaunias, *J. Non-Cryst. Solids* **153-154**, 312 (1993).
- ²⁰A. Sadoc, E. Belin, Z. Danhkázi, and A.M. Flank, *J. Non-Cryst. Solids* **153-154**, 338 (1993).
- ²¹A. Sahnoune, J.O. Ström-Olsen, Z. Altounian, C.C. Homes, T. Timusk, and X. Wu, *J. Non-Cryst. Solids* **153-154**, 343 (1993).
- ²²A. Shastri, F. Borsa, A.I. Goldman, J.E. Shield, and D.R. Torgeson, *J. Non-Cryst. Solids* **153-154**, 347 (1993).
- ²³K. Wang, C. Scheidt, P. Garoche, and Y. Calvayrac, *J. Non-Cryst. Solids* **153-154**, 357 (1993).
- ²⁴G. Coddens, R. Bellissent, Y. Calvayrac, and J.P. Ambroise, *Europhys. Lett.* **16**, 271 (1991).
- ²⁵G. Coddens and R. Bellissent, *J. Non-Cryst. Solids* **153-154**, 557 (1993).
- ²⁶T. Klein, G. Pares, J.-B. Suck, G. Fourcaudot, and F. Cyrot-Lackmann, *J. Non-Cryst. Solids* **153-154**, 562 (1993).
- ²⁷M. Quilichini, B. Hennion, and G. Heger, *J. Non-Cryst. Solids* **153-154**, 568 (1993).
- ²⁸G. Coddens, C. Soustelle, R. Bellissent, and Y. Calvayrac, *Europhys. Lett.* **23**, 33 (1993).
- ²⁹S.S. Kang and J.M. Dubois, *Philos. Mag. A* **66**, 151 (1992).
- ³⁰U. Köster, W. Liu, H. Liebertz, and M. Michel, *J. Non-Cryst. Solids* **153-154**, 446 (1993).
- ³¹L. Bresson and D. Gratias, *J. Non-Cryst. Solids* **153-154**, 468 (1993).
- ³²F.S. Pierce, P.A. Bancel, B.D. Biggs, Q. Guo, and S.J. Poon, *Phys. Rev. B* **47**, 5670 (1993).
- ³³P. Lindqvist, C. Berger, T. Klein, P. Lanco, F. Cyrot-Lackmann, and Y. Calvayrac, *Phys. Rev. B* **48**, 630 (1993).
- ³⁴T. Klein, C. Berger, D. Mayou, and F. Cyrot-Lackmann, *Phys. Rev. Lett.* **66**, 2907 (1991).
- ³⁵R.A. Dunlap, D.W. Lawther, and R.H. March, *J. Phys. F* **17**, L39 (1987).
- ³⁶M.K. Sanyal, P.M.G. Nambissan, R. Chidambaram, and P. Sen, *J. Phys. Condens. Matter* **1**, 3733 (1989).
- ³⁷T. Kizuka, I. Kanazawa, Y. Sakurai, S. Nanao, H. Murakami, and T. Iwashita, *Phys. Rev. B* **40**, 796 (1989).
- ³⁸R. Chidambaram, M.K. Sanyal, P.M.G. Nambissan, and P. Sen, *J. Phys. Condens. Matter* **2**, 251 (1990).
- ³⁹I. Kanazawa, T. Kizuka, M. Ohata, Y. Sakurai, S. Nanao, and T. Iwashita, *J. Non-Cryst. Solids* **117-118**, 793 (1990).
- ⁴⁰I. Kanazawa, T. Iwasita, T. Ohata, S. Nanao, and S. Takeuchi, *Mater. Sci. Forum* **105-110**, 1093 (1992).
- ⁴¹R. Chidambaram, M.K. Sanyal, P.M.G. Nambissan, and P. Sen, *Bull. Am. Phys. Soc.* **35**, 331 (1990).
- ⁴²T. Ohata, I. Kanazawa, T. Iwashita, K. Kishi, and S. Takeuchi, *Phys. Rev. B* **42**, 6730 (1990).
- ⁴³D. Shi, L.Y. Xiong, and W. Deng, *Mater. Sci. Forum* **105-110**, 829 (1992).
- ⁴⁴D.W. Lawther, G. Beydaghyan, and R.A. Dunlap, *J. Phys. Condens. Matter* **2**, 6239 (1990).
- ⁴⁵R. Chidambaram, M.K. Sanyal, P.M.G. Nambissan, and P. Sen, *J. Phys. Condens. Matter* **2**, 9941 (1990).
- ⁴⁶R.H. Howell, C. Berger, F. Solal, Y. Calvayrac, and P.E.A. Turchi, *Mater. Sci. Forum* **105-110**, 651 (1992).
- ⁴⁷K. Kristiaková, S. Mäkinen, J. Kristiak, and D. Janickovic, *Mater. Sci. Forum* **105-110**, 1113 (1992).
- ⁴⁸D.W. Lawther and R.A. Dunlap, *J. Non-Cryst. Solids* **153-154**, 611 (1993).
- ⁴⁹D.W. Lawther and R.A. Dunlap, *Key Eng. Mat.* **81-83**, 95 (1993).
- ⁵⁰R. Chidambaram, M.K. Sanyal, V.S. Raghunathan, P.M.G. Nambissan, and P. Sen, *Phys. Rev. B* **48**, 3030 (1993).
- ⁵¹V. Elser and C.L. Henley, *Phys. Rev. Lett.* **55**, 2883 (1985).
- ⁵²M. Audier, P. Sainfort, and B. Dubost, *Philos. Mag. B* **54**, L105 (1986).
- ⁵³P.W. Stephens and A.I. Goldman, *Phys. Rev. Lett.* **56**, 1168 (1986).
- ⁵⁴J.E. Shield, M.J. Kramer, R.W. McCallum, and A.I. Goldman, in *Physics and Chemistry of Finite Systems: From Clusters to Crystals*, edited by P. Jena *et al.* (Kluwer Academic, Amsterdam, 1992), Vol. I, p. 125.
- ⁵⁵T. Ishimasa and M. Mori, *Philos. Mag. Lett.* **62**, 357 (1990).
- ⁵⁶P. Kirkegaard and M. Eldrup, *Comput. Phys. Commun.* **7**, 401 (1974).
- ⁵⁷A. Seeger, F. Banhart, and W. Bauer, in *Positron Annihilation*, edited by L. Dorikens-Vanpraet, M. Dorikens, and D. Segers (World Scientific, Singapore, 1989), p. 275.
- ⁵⁸S.E. Burkov, T. Timusk, and N.W. Ashcroft, *J. Phys. Condens. Matter* **4**, 9447 (1992).
- ⁵⁹The value of $|\mathbf{G}| = 3.094 \text{ \AA}^{-1}$ is calculated from a weighted average of the reciprocal vectors, $|\mathbf{G}|_{422222} (=2.9856 \text{ \AA}^{-1})$ and $|\mathbf{G}|_{442002} (=3.1381 \text{ \AA}^{-1})$, corresponding to the 422222 and 442002 x-ray powder diffraction peaks. The weighting corresponds to the multiplicity of the Bragg planes: 12 planes normal to the five-fold axes of the icosahedron for the 422222 peak; and 30 planes oriented along the two-fold edges of the icosahedron for the 442002 peak. Thus $|\mathbf{G}| = (12/42)|\mathbf{G}|_{422222} + (30/42)|\mathbf{G}|_{442002}$.
- ⁶⁰L. Pauling, *Phys. Rev.* **54**, 899 (1938).
- ⁶¹A. Seeger and F. Banhart, *Phys. Status Solidi A* **102**, 171 (1987).
- ⁶²F. Dénoyer, G. Heger, M. Lambert, M. Audier, and P. Guyot, *J. Phys. (Paris)* **51**, 651 (1990).
- ⁶³T. Motsch, F. Dénoyer, P. Launois, and M. Lambert, *J. Phys. (France) I* **2**, 861 (1992).
- ⁶⁴R.M. Nieminen, in *Positron Solid-State Physics*, edited by W. Brandt and A. Dupasquier (North-Holland, Amsterdam, 1983), p. 359.
- ⁶⁵P. Hautojarvi, J. Heinio, M. Manninen, and R. Nieminen, *Philos. Mag.* **35**, 973 (1977).